# Structural Studies on ADP Activation of Mammalian Glutamate Dehydrogenase and the Evolution of Regulation[†,‡]

Soojay Banerjee,[§] Timothy Schmidt,[||] Jie Fang,[⊥] Charles A. Stanley,[⊥] and Thomas J. Smith*[,§]

*Donald Danforth Plant Science Center, St. Louis, Missouri 63132, Department of Biological Sciences, Purdue University, West Lafayette, Indiana 47907, and The Children's Hospital of Philadelphia, Endrocrinology Division, Room 410D, 3516 Civic Center Boulevard, Philadelphia, Pennsylvania 19104*

*Received December 9, 2002; Revised Manuscript Received January 27, 2003*

ABSTRACT: Glutamate dehydrogenase (GDH) is found in all organisms and catalyzes the reversible oxidative deamination of L-glutamate to 2-oxoglutarate. Unlike GDH from bacteria, mammalian GDH exhibits negative cooperativity with respect to coenzyme, activation by ADP, and inhibition by GTP. Presented here are the structures of apo bovine GDH, bovine GDH complexed with ADP, and the R463A mutant form of human GDH (huGDH) that is insensitive to ADP activation. In the absence of active site ligands, the catalytic cleft is in the open conformation, and the hexamers form long polymers in the crystal cell with more interactions than found in the abortive complex crystals. This is consistent with the fact that ADP promotes aggregation in solution. ADP is shown to bind to the second, inhibitory, NADH site yet causes activation. The $\beta$-phosphates of the bound ADP interact with R459 (R463 in huGDH) on the pivot helix. The structure of the ADP-resistant, R463A mutant of human GDH is identical to native GDH with the exception of the truncated side chain on the pivot helix. Together, these results strongly suggest that ADP activates by facilitating the opening of the catalytic cleft. From alignment of GDH from various sources, it is likely that the antenna evolved in the protista prior to the formation of purine regulatory sites. This suggests that there was some selective advantage of the antenna itself and that animals evolved new functions for GDH through the addition of allosteric regulation.

Glutamate dehydrogenase (GDH, EC 1.4.1.2) is found in all organisms and catalyzes the reversible oxidative deamination of L-glutamate to 2-oxoglutarate. GDH from mammalian sources utilizes NAD(H) and NADP(H) as coenzymes with comparable efficacies. The enzyme is a homohexamer with each subunit having a molecular mass of ~56 kDa. The structures of GDH from bovine (boGDH)[1] (*1*, *2*), human (huGDH) (*3*), and several bacterial sources (*4*−*7*) have been determined using X-ray crystallography. The core structure of the enzyme is a stacked dimer of trimers of the N-terminal, "glutamate-binding domain" that is composed mostly of $\beta$-strands. On top of these domains are the NAD binding domains that rotate down upon substrate and coenzyme to initiate catalysis. This rotation occurs about a helix at the back of the NAD binding domain called the "pivot helix". Unlike bacterial GDH, a 48-residue "antenna" extends from the top of the NAD binding domain. The antennae from the three subunits within the trimers wrap around each other and undergo conformational changes as the catalytic mouth opens and closes (*3*).

Unlike bacterial GDH, mammalian GDH is allosterically regulated by a number of small molecules including GTP, ADP, leucine, and coenzyme (*8*). The two major, opposing allosteric regulators, ADP and GTP, appear to exert their effects via abortive complexes [NAD(P)H·GLU and NAD(P)·αKG] (*9*−*11*). ADP is an activator believed to act, at least in part, by destabilizing abortive complexes (*9*, *10*) and abrogating negative cooperativity (*12*). In contrast, GTP is a potent inhibitor thought to act by stabilizing abortive complexes (*11*). GTP binding is antagonized by phosphate (*13*) and ADP (*14*) but is synergistic with NADH bound in the noncatalytic site (*13*).

The structures of several key GDH complexes have been determined to date: boGDH·GLU·NAD(P)H·GTP (*2*, *15*), boGDH·αKG·$NAD^+$ (*2*), and apo huGDH (*3*). From these structures, it was found that the inhibitor, GTP, binds at the junction between the NAD binding domain and the antenna. The majority of the contacts between GTP and the enzyme are via the triphosphate moiety and suggest that this allosteric site might be an "energy sensor" that turns the enzyme off when the cell is at a high energy state.

NADH has been shown to bind to a second site on each subunit, but the effect of coenzyme binding to this site is unclear (*3*). This second coenzyme site binds NAD(H) ~10-fold better than NADP(H) (*16*, *17*) with the reduced forms binding better than the oxidized forms (*18*). It has been suggested that reduced coenzyme at this site inhibits the

[†] This work was supported by grants from the National Institutes of Health (GM10704) to T.J.S. and from the American Diabetes Association to C.A.S. and T.J.S. (1320000179).

[‡] The apo boGDH, boGDH·ADP, and R463A huGDH structures have been deposited in the Protein Data Bank and have the accession designations of 1NR7, 1NQT, and 1NR1, respectively.

* Corresponding author. Tel: (314) 587-1451. Fax: (314) 587-1551. E-mail: tsmith@danforthcenter.org.

[§] Donald Danforth Plant Science Center.

[||] Purdue University.

[⊥] The Children's Hospital of Philadelphia.

[1] Abbreviations: boGDH, bovine glutamate dehydrogenase; huGDH, human glutamate dehydrogenase; HI/HA, hyperinsulinism/hyperammonemia; PEG, poly(ethylene glycol); TEM, transmission electron microscopy.

10.1021/bi0206917 CCC: $25.00 
Published on Web 03/05/2003

reaction (*16*, *17*) while oxidized coenzyme binding causes activation (*19*). Recent studies on several boGDH complexes have shown that NAD(H), but not NADP(H), binds to this second site (*2*). The area to which NADH binds is in the region that has been identified as the ADP binding site from chemical modification studies using reactive ADP analogues (*20*). Furthermore, a model has been proposed whereby $_h$R463 (R459 in boGDH) on the pivot helix interacts with the bound ADP and leads to activation of the enzyme by facilitating the opening of the active site cleft (*2*). For clarity, the h and b prefixes will be used to designate human and bovine sequence numbering, respectively. This model was supported by an $_h$R463A mutation in huGDH that abrogated ADP activation (*2*, *21*). These studies also suggested that NADH inhibition might not be due to reduced coenzyme binding to this site since it was not clear how $NAD^+$ binding to the same site could cause opposite effects.

Clues as to the physiological roles of GDH in mammals and its allosteric regulation have been recently revealed by the finding that the hyperinsulinism/hyperammonemia (HI/HA) syndrome in humans is caused by defects in GDH regulation (*22*, *23*). Patients with this disorder are heterozygous for mutant forms of GDH that are unresponsive to the inhibitor, GTP. The results from these studies suggested that GDH mainly operates in the oxidative deamination reaction in the pancreas and liver and may be involved in insulin homeostasis. While most of these mutations lie within the GTP binding pocket, a number reside on the antenna and are not directly involved in GTP binding. However, these mutations are predicted to affect the stability of a short helix on the descending strand of the antenna, and this suggests that the antenna is involved in the process of GTP inhibition (*3*).

Presented here are the structures of boGDH in the presence or absence ADP and of the R463A mutant form of huGDH. We find that ADP binds in the same location as the adenosine ribose moiety of NADH. However, its orientation is not identical to that of NADH and may be a consequence of the lack of the nicotinamide ribose moiety. The orientation of the NAD binding domain is not identical among the 12 subunits in the asymmetric unit but is correlated to antenna conformation. This suggests that the antennae within the trimer can exist in multiple conformational states. In most of the subunits $_b$R459 is observed to interact with the $\beta$-phosphate of ADP. This supports our previous contention that, unlike GTP, ADP can bind to the open and closed forms of the enzyme and $_b$R459 interacts with ADP in the open conformation and this results in activation. Furthermore, the structure of the $_h$R463A mutation that abrogates ADP activation clearly shows that the effect of this mutation is limited to the truncation of the side chain. With the locations of the allosteric sites identified, sequence alignments among samples of all five phylogenetic kingdoms suggest that the antenna appeared before the purine regulatory sites as members of the protista (paramecium) started to evolve into multicellular animals. All members of the animal kingdom appear to have both the antenna and regulatory regions. These results are discussed in the context of differing roles of GDH in various organisms.

## MATERIALS AND METHODS

*Structure Determination of Apo boGDH.* Apo boGDH crystals were prepared using the vapor diffusion method and sitting drop apparatus. The enzyme was purchased from Boeringer-Mannheim as a 50% glycerol suspension. The enzyme was dialyzed extensively against 0.1 M sodium phosphate buffer, pH 6.7−6.8, and adjusted to a concentration of 10 mg/mL. The reservoir solution contained 10% PEG 8000 (w/v), 0.8 M sodium chloride, 4% methylpentanediol (v/v), 1 mM sodium azide, 0.1 M sodium phosphate buffer, pH 6.7−6.8, and 0.75−1.5% octyl $\beta$-glucopyranoside (w/v). The drop volume was comprised of 22.5 $\mu$L of reservoir solution and 7.5 $\mu$L of enzyme solution. Crystals formed within 2 weeks and grew for an additional 2 weeks. The crystals were prepared for freezing in the Oxford system cryostream by incubation in a synthetic mother liquor solution containing increasing concentrations of glycerol. This solution contained 0.1 M sodium phosphate, 1% octyl $\beta$-glucopyranoside (w/v), 6% methylpentanediol (v/v), 1 M sodium phosphate, 14% PEG 8000 (w/v), and 1 mM sodium azide. The crystals were incubated for 30 min in each of the solutions containing 0%, 2%, 5%, and 10% glycerol (v/v). At the end of these incubations, the concentration of PEG 8000 in the synthetic mother liquor was increased to 22%, and the crystals were incubated for 30 min in each of the solutions containing 12.5%, 15%, 17.5%, and 20% glycerol. Data were collected on an Raxis IV imaging plate system attached to a Rigaku generator from a single crystal with dimensions of 0.3 mm × 0.3 mm × 0.1 mm. A total of 200 images were collected using an oscillation angle of 0.4° and exposure time of 45 min. The crystals belonged to the $P2_12_12_1$ space group with unit cell dimensions of $a = 96.6$ Å, $b = 172.1$ Å, and $c = 441.0$ Å. Diffraction data to 3.5 Å (Table 1) were used for the structure determination.

Table 1: Data and Refinement Statistics

| | apo boGDH | boGDH/ADP | R463A huGDH |
|---|---|---|---|
| resolution range (Å) | 20−3.3 | 20−3.5 | 20−3.3 |
| redundancy | 2.4 (1.6) | 2.3 (1.6) | 1.4 (1.3) |
| completeness (%) | 74.5 (43.1) | 70.7 (49.6) | 64.6 (62.9) |
| $I/\sigma$ | 15.0 (4.1) | 18.0 (4.0) | 13.8 (2.3) |
| $R$-factor (%) | 4.4 (11.0) | 4.0 (11.1) | 3.2 (13.7) |
| model $R_{work}$ (%) | 21.2 (27.3) | 20.7 (26.4) | 22.6 (28.3) |
| model $R_{free}$ (%) | 29.2 (36.7) | 27.6 (35.0) | 27.6 (33.6) |
| RMS bond error (Å) | 0.01 | 0.016 | 0.017 |
| RMS angular error (deg) | 1.26 | 1.92 | 1.98 |
| Ramachandran | | | |
| % favored | 80.8 | 74.4 | 79.6 |
| % additional | 16.9 | 21.9 | 17.4 |
| % generous | 1.9 | 3.1 | 2.0 |
| % disallowed | 0.5 | 0.6 | 1.0 |

The structure was determined using the molecular replacement method and the structure of apo huGDH (*3*) as a starting model. From $V_m$ calculations (*24*), it was determined that there were two hexamers of GDH in each asymmetric unit ($V_m = 2.7$ Å$^3$/Da). The program CNS (*25*) was used for both the rotation and translation function searches. Reflections between 15 and 4 Å were used for structure determination. The cross-rotation function showed a dominant peak with a height/sigma of ∼10. One copy of the huGDH hexamer was fixed at this orientation, and the cross-rotation function was run again to find the second hexamer. This yielded a second peak of comparable height. These two solutions were then used for the translation function, and this yielded two clear solutions as well. The initial $R$-factor for this model was 32%. This model was then subjected to 30 steps of rigid body

refinement without NCS restraints and then energy minimization with and without NCS restraints. Simulated annealing was then applied at a temperature of 2500 K with NCS restraints, followed by energy minimization and individual *B* value refinement. This model was rebuilt using the program "O" and further refined with CNS. The final model, with NCS restraints applied, has an RMS deviation in bond length of 0.001 Å and an RMS deviation in bond angle of 1.26°. The final statistics are summarized in Table 1.

*Structure Determination of the boGDH/ADP Complex.* For the boGDH/ADP complex, boGDH was crystallized in the absence of any ligands as described above, and then ADP was diffused into the crystals. It is possible that the conformation of the enzyme is restricted by the crystalline contacts. However, this seems unlikely since soaking coenzyme and/or glutamate into crystals causes rapid disintegration. Therefore, in the case of GDH, if ligand binding causes conformational changes, the crystals are destroyed rather than the lattice constraining conformational changes. The only difference in crystallization and freezing protocols was that the synthetic mother liquor used for preparing the crystals for freezing contained 0.1 M sodium phosphate, 1% octyl $\beta$-glucopyranoside (w/v), 6% methylpentanediol (v/v), 1 M sodium phosphate, 14% PEG 8000 (w/v), 1 mM sodium azide, and 0.3 mM ADP. Data were collected on an Raxis IV imaging plate system attached to a Rigaku generator from a single crystal with dimensions of 0.42 mm × 0.13 mm × 0.24 mm. A total of 200 images were collected using an oscillation angle of 0.4° and exposure time of 45 min. The crystals belonged to the $P2_12_12_1$ space group with unit cell dimensions of $a = 96.4$ Å, $b = 172.2$ Å, and $c = 439.9$ Å, and diffraction data were used to a resolution of 3.5 Å (Table 1). Since these crystals were isomorphous to those of apo boGDH, the apo boGDH structure was used directly for this structure determination and refined using CNS and O. The final model has an RMS deviation in bond length of 0.016 Å and RMD deviation in bond angle of 1.92°. The refinement results are further summarized in Table 1.

*Structure Determination of the R463A huGDH Mutant.* The R463A mutant of human GDH was cloned, expressed, and purified as previously described (*21*). R463A GDH crystals were prepared using the vapor diffusion method and sitting drop apparatus. The enzyme was dialyzed against 0.1 M sodium phosphate, pH 6.8, and adjusted to a concentration of 26 mg/mL. The reservoir solution contained 10% PEG 8000 (w/v), 0.1 M sodium chloride, 1.3% octyl $\beta$-glucopyranoside (w/v), 7.5% methylpentanediol (v/v), 0.1 M sodium phosphate, pH 6.8, and 1 mM sodium azide. The drop was composed of 8 $\mu$L of reservoir, 1.35 $\mu$L of enzyme solution, and 0.65 $\mu$L of water. The crystals were prepared for freezing in a manner similar to that for the boGDH crystals with the exception that the synthetic mother liquor had lower concentrations of sodium phosphate and sodium chloride (60 and 50 mM, respectively) and a higher concentration of methylpentanediol [8% (v/v)]. Data were collected from a single crystal with dimensions of 0.22 mm × 0.24 mm × 0.11 mm on the same X-ray source as described above. The data set is composed of 265 diffraction images with oscillation angles of 0.4° and exposure times of 45 min (Table 1). The crystal belonged to the space group *P*1 and had unit cell parameters of $a = 96.92$ Å, $b = 98.57$ Å, $c = 124.05$ Å, $\alpha = 86.56°$, $\beta = 69.79°$, and $\gamma = 60.99°$ (Table 1).

Since this unit cell was nearly identical to that of the previously characterized native huGDH crystals (*3*), molecular replacement was used to determine this structure. CNS (*25*) and O were used for refinement and model building, respectively. The final model has an RMS deviation in bond length and angle of 0.017 Å and 1.98°, respectively. The final refinement statistics are summarized in Table 1.

## RESULTS

*Polymer Formation in the Crystal Cell.* boGDH undergoes a reversible polymerization process (*26*−*28*). ADP is an agonist whereas NADH and GTP are antagonists of this process (*16*, *17*, *29*). Shown in Figure 1 is the linear array of hexamers observed in crystals of the "closed", abortive complex form of the enzyme. Most of the contacts between these hexamers are made by the antenna regions. In the apo form, the hexamers interact at an angle to each other such that the antenna of one interacts with the top of the NAD domain and the antenna of the adjacent hexamer. Compared to the polymers observed in the closed mouth conformers, these polymers have a more helical arrangement in the crystal cell. Using the program MS (*30*−*32*) and a 1.7 Å probe radius, the surface area at the interface is 680 Å$^2$ and 1642 Å$^2$ for the complexed and apo forms, respectively.

*Subunit Conformations.* In the apo boGDH and the boGDH/ADP crystals, there are 12 independent subunits in the asymmetric unit. As with the previous huGDH structure (*3*), it was immediately apparent that the NAD binding domains were not in identical orientations. In the GDH hexamer, the first ∼150 residues of the subunits form the core structure that is unaffected by the opening of the catalytic cleft. Therefore, this domain was used to align all 12 subunits in order to isolate differences in the NAD binding domain (Figure 2). From this figure, it is clear that the NAD binding domain can sample a wide range of conformations within the hexamer.

*ADP Binding Environment.* The electron density for ADP was immediately apparent when phases were derived from the initial model that did not include the structure of ADP (Figure 3). ADP binds behind the NAD binding domain, just beneath the pivot helix. The adenosine moiety binds down into a fairly hydrophobic pocket with the ribose phosphate groups pointing up toward the pivot helix. In particular, with the catalytic mouth open, $_b$R459 from the pivot helix reaches down and binds to the $\beta$-phosphates of the bound ADP.

However, these and other interactions between ADP and the pivot helix differ among the 12 subunits in the asymmetric unit because of differences in the orientation of the NAD binding domains (Table 2). In the apo boGDH model, the catalytic cleft opening varies by ∼5°. The difference in cleft opening is roughly correlated with distance between R459 and the phosphates of ADP. For example, the A3 subunit has the greatest cleft opening and the closest R459/ADP interactions while subunit A5 has the most closed conformation and R459 does not make contact with the bound ADP. For comparison, the catalytic cleft in the abortive complex (*2*) is ∼7° more closed than subunit A5.

*Comparison between NADH and ADP Bound to the ADP Site.* The previous structures of the boGDH·GLU·NADH·GTP, boGDH·GLU·NADPH·GTP, and boGDH·αKG·NAD$^+$ complexes have shown that NAD(H), but not NADPH, binds

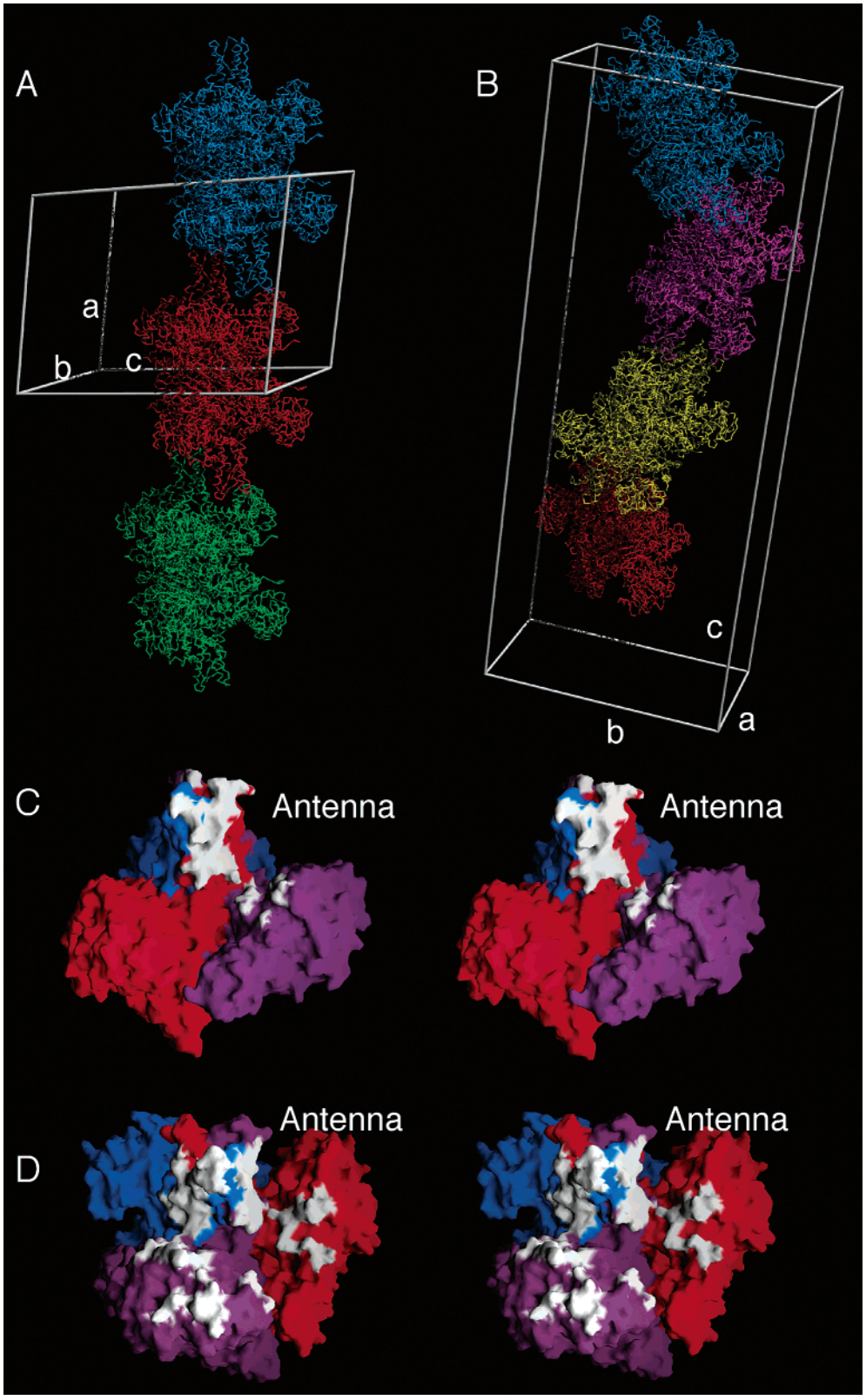


FIGURE 1: Polymers of GDH observed in crystals of apo and abortive complex forms of GDH. Shown at the top are the polymers of boGDH as found in the NADH·GLU·GTP (A) and ADP complexes (B). The white lines indicate the boundaries of one unit cell with the three axes labeled. Different hexamers are represented in varying colors. In (A), there is one hexamer in the *P*21 asymmetric unit, and these polymers lie parallel to the *a* axis. In (B), there are two hexamers in the asymmetric unit. One pair is shown in red and yellow and the other in mauve and blue. Here the chain of hexamers lies along the *c* axis of the $P2_12_12_1$ cell. Shown in (C) is a stereo diagram of the NADH·GLU·GTP/boGDH trimer contact surface as calculated by MS (*31*, *32*) using a 1.7 Å probe radius. The three different subunits are shown in different colors, and the area contacted by the adjacent hexamer along the fiber is shown in white. Similarly, the area contacted by the adjacent hexamer in the chains observed in the ADP/boGDH complex is shown in (D).

to the same site as ADP (*2*). In these structures, the nicotinamide ribose moiety is observed to be oriented in two different conformers: pointing down into the subunit interface within the trimer and pointing up toward the pivot helix.

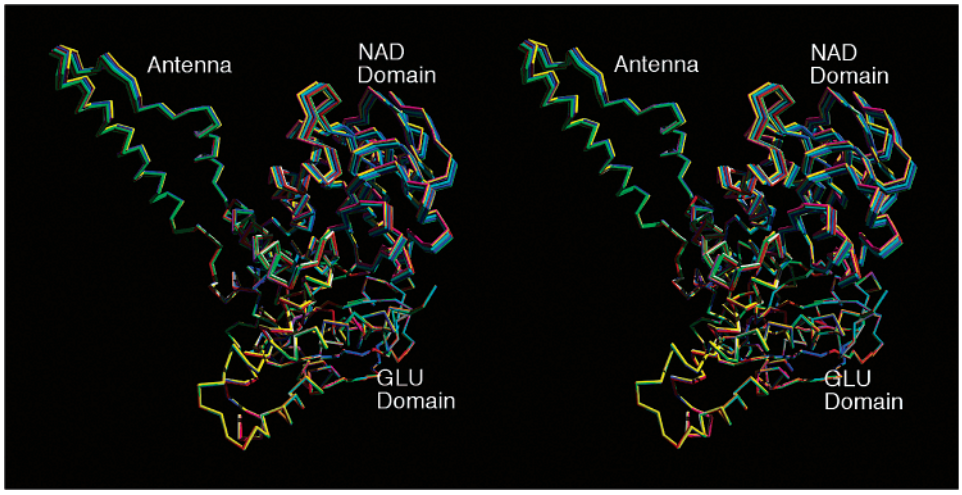


FIGURE 2: Differences in the NAD binding domain conformation among the 12 subunits found in the crystallographic asymmetric unit. Shown here is a C-α backbone stereo diagram of the 12 subunits aligned according to the GLU binding domains. The colors used range from red to purple as the subunit identification varies from A1 to B6 (the A and B designate the hexamer). Note that there is a wide range of antenna and NAD binding domain conformations among the 12 subunits and that the antenna and NAD binding domains move toward each other as the catalytic cleft opens.

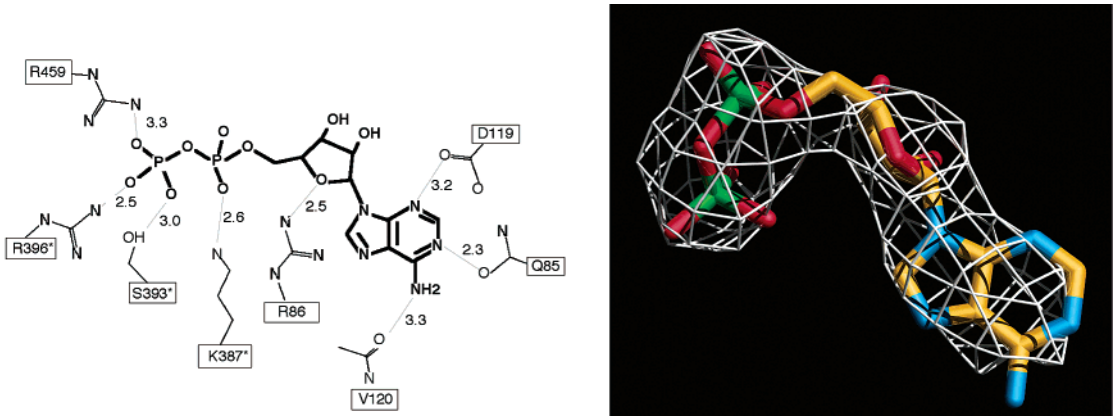


FIGURE 3: Electron density and binding environment of ADP. On the left is a schematic diagram of the charge and polar interactions between the bound ADP and boGDH. On the right is the model of the bound ADP fitted into the electron density. The electron density shown here is a $2F_o - F_c$ omit map contoured at $1\sigma$. The carbon, nitrogen, oxygen, and phosphorus atoms are colored yellow, blue, red, and green, respectively.

Table 2: Differences in ADP Contacts among the 12 Subunits in the Asymmetric Unit[a]

| ADP no. | Arg459[1] | Arg396[1*] | Ser393[1] | Lys387[1*] | Asp119[2] | Arg86[2] | Gln85[3] | Pro120[3] MC carbonyl | angle |
|---|---|---|---|---|---|---|---|---|---|
| A1 | 3.30 | 2.50 | 3.00 | 2.60 | 3.20 | 2.50 | 2.30 | 3.30 | 73.5 |
| A2 | 3.40 | 3.10 | 2.90 | 2.50 | 3.30 | 3.00 | 2.60 | 3.50 | 73.6 |
| A3 | 2.70 | | 3.60 | 2.60 | 3.20 | 3.00 | 2.50 | 3.60 | 76.8 |
| A4 | 2.70 | 3.70 | 3.10 | 2.60 | 4.10 | 2.40 | 2.70 | 2.90 | 74.1 |
| A5 | 3.70 | 2.90 | 2.70 | 2.50 | 3.70 | 2.60 | 2.70 | 3.70 | 71.2 |
| A6 | 2.50 | 3.20 | 2.80 | 2.80 | 3.40 | 2.80 | 2.90 | 3.10 | 74.2 |
| B1 | 3.00 | 2.70 | 3.00 | 2.70 | 3.90 | 2.80 | 3.30 | 3.80 | 73.0 |
| B2 | 2.70 | 2.90 | | 2.60 | 3.40 | 3.70 | 2.80 | 3.90 | 74.2 |
| B3 | 2.60 | 3.10 | 3.80 | 2.80 | 3.90 | 2.90 | 3.20 | 3.20 | 75.7 |
| B4 | 2.60 | 2.80 | 2.90 | 3.00 | 3.70 | 2.80 | 2.40 | 3.20 | 72.5 |
| B5 | 2.60 | 3.10 | 2.60 | 2.60 | 3.50 | 2.70 | 2.60 | 3.20 | 73.5 |
| B6 | 3.40 | 3.50 | 3.70 | 2.80 | 3.70 | 2.70 | 2.80 | 3.00 | 73.9 |
| AV | 2.93 | 3.05 | 3.10 | 2.68 | 3.58 | 2.83 | 2.73 | 3.37 | 73.9 |
| (SD) | (0.41) | (0.34) | (0.41) | (0.15) | (0.29) | (0.33) | (0.30) | (0.33) | (1.42) |

[a] All distances are measured in angstroms. Superscripts 1, 2, and 3 define the binding region of ADP in contact with the enzyme (1, phosphate; 2, sugar; 3, base). The superscript * indicates that the contact is made with the adjacent subunit. The α and $\beta$ notations designate the phosphate group. MC designates a main chain contact. The angle between the domains was calculated using the dot product of the vectors between the center of masses of the GLU binding domain (residues 50−150), the NAD binding domain (residues 220−367), and the pivot helix (residues 445−469). The last two rows show the average distance (AV) and the standard deviation (SD).

As shown in Figure 4, while the general binding site is the same for NAD(H) and ADP, the details of binding differ between these ligands.

*huGDH R463A Mutant Structure*. In previous studies, it was shown that the R463A mutation in huGDH abrogates ADP activation (*21*). It was suggested that $_h$R463 on the pivot


FIGURE 4: Differences between NADH and ADP binding to the ADP site. Shown here is a stereo diagram of one subunit of boGDH with the bound NADH and ADP represented as stick figures. The view is with antenna (shown in orange) and the 3-fold axis of the enzyme lying vertically on the left side. The GLU binding domain is shown in green, the $NAD^+$ binding domain in mauve, and the pivot helix in blue. The white box on the top part of the figure denotes the area that is magnified at the bottom of the figure. For this figure, the GLU binding domains of the ADP/boGDH and the NADH·GLU·GTP/boGDH complexes were aligned, and the coordinates of the NADH molecule (white stick) bound to the second site were laid on top of the ADP complex with the ADP represented as a multicolor stick figure. Note that while the ADP moieties of both compounds bind to the same site, they do so with different conformations.

helix interacts with bound ADP when the catalytic mouth opens (*3*). Therefore, the loss of this side chain might abrogate activation but not necessarily ADP binding. Alternatively, this mutation could block ADP binding by altering the structure of the ADP site. To test these possibilities, the structure of the huGDH R463A mutant was determined. As shown in Figure 5, the effect of this R463A mutation is limited to $_h$R463. The electron density clearly shows the loss in the side chain density for this residue, and there are no significant deviations in the pivot helix backbone.

*Evolution of GDH Regulation.* The structures of the various mammalian GDH complexes have clearly defined where the allosteric regulators bind and that the antenna moves as the catalytic cleft opens and closes. However, it is not clear how the antenna and these regulatory sites interact nor are the physiological roles of these features well understood. One way to address these issues is to examine the amino acid sequences of GDH's from a variety of sources to ascertain when these features evolved. For these comparisons, the structures were used for sequence alignments (*15*) and by BLAST (*33*) when the structures were not available.

The first region examined was the antenna domain (Table 3). Interestingly, bacteria, fungi, and plants do not have this feature. The antenna first appears in the most primitive animal-like organisms, the protozoa (paramecium) of the protista kingdom. However, the antenna in paramecium is seven residues shorter compared to multicellular animals and is only 27% identical in sequence to boGDH. Further up the phylogenetic tree, nematodes have antennae that are only three residues shorter than, and more homologous (~50%) to, boGDH. Insects have antennae that are the same length as boGDH and are nearly identical in sequence (~80%). The most unusual finding in insects was that *Drosophila* have at least two forms of GDH with one being 13 residues longer in the antenna region than any other GDH sequenced to date (*34*). This insertion lies within the ascending helix of the antenna and appears to be a duplication of a section of this helix. Most secondary structure prediction algorithms predict this insertion to greatly elongate the length of this helix. It is not clear what the role of this elongated antenna is, but this form of GDH is expressed at 10% or less of the total GDH in tissue (*34*). Further up the evolutionary tree, multicellular animals all appear to have basically identical antennae.

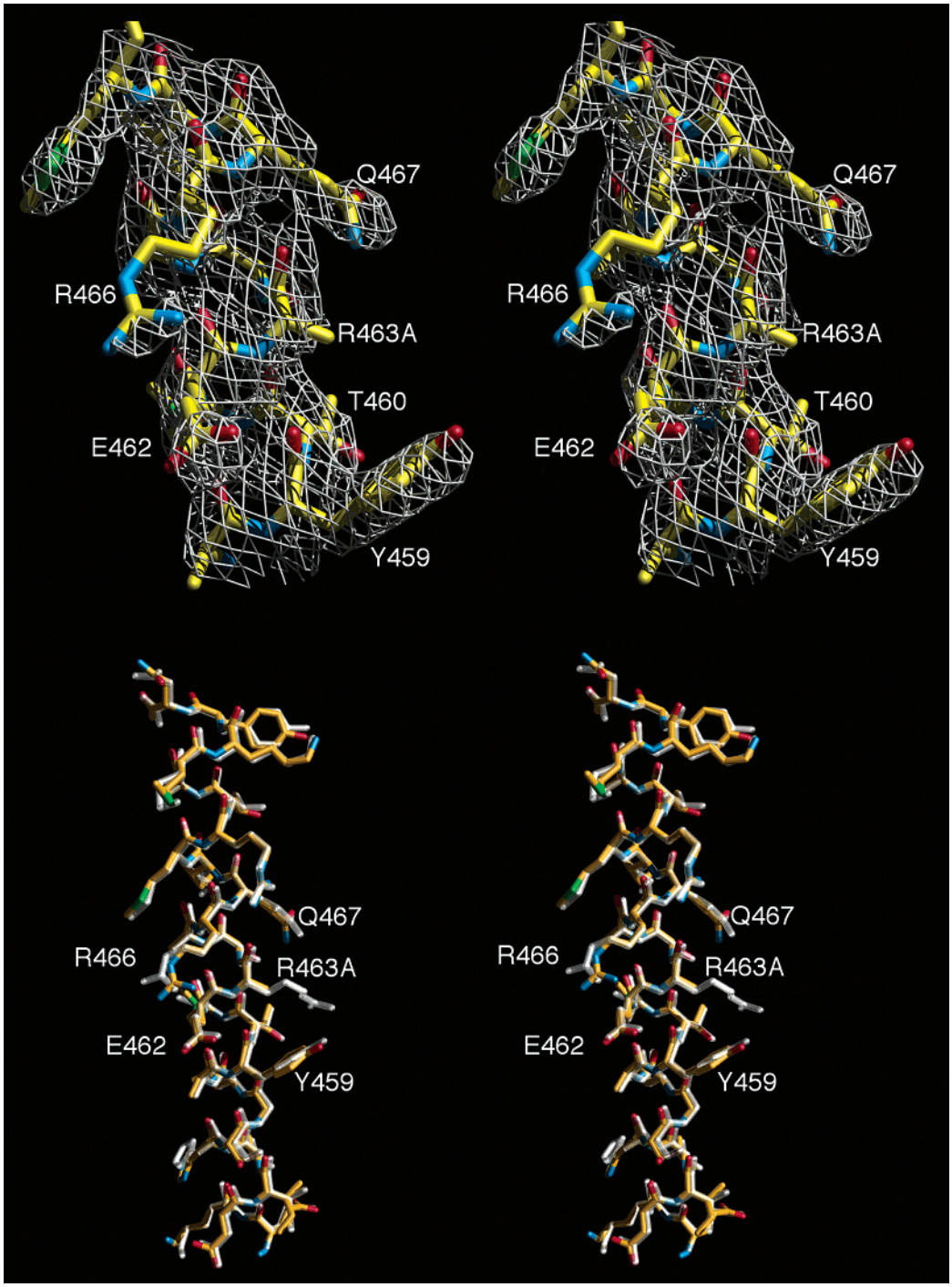


FIGURE 5: Effects of the R463A mutation on huGDH. The top stereo diagram shows the atomic model of the huGDH R463A structure, represented as a stick figure, modeled into the electron density, represented as a white cage. The approximate orientation is looking down from the top of the subunit with the 3-fold axis of the enzyme coming out of the bottom of the diagram. The stereopair on the bottom of the figure shows a comparison between this helix as observed in the native (transparent white structures) and mutant (stick figures colored according to atom type) structures.

The inhibitory GTP site appears to be unique to the animal kingdom. Shown in Table 4 is a list of the residues that form the lining of the GTP binding pocket. It is clear from this table that a number of these residues found in the protista, fungi, plant, and monerans would prevent GTP binding. Using the boGDH sequence numbering, S213 interacts with a ribose hydroxyl. This serine is replaced by a glutamate in members from these other kingdoms. R265 and R217 that interact with the $\gamma$-phosphate of GTP in animal GDH is, in most cases, replaced by hydrophobic or acidic residues in these other life forms. Finally, it is known that a H454Y mutation in huGDH (H450 in boGDH) abrogates GTP inhibition in the HI/HA syndrome (*35*). This histidine is not conserved in these other kingdoms. Together, these residues are not likely to form a pocket that permits GTP binding.

The results of the alignment of the ADP sites are less striking than those observed in the case of the GTP site (Table 5), but it seems likely that ADP regulation only occurs in animals. Among the GDH's from the non-animal kingdom sources, paramecium GDH appears to be the most homolo-

Table 3: Alignment of the Antenna Domains from Various Organisms[a]

```
          400       410                   420       430       440
GRLTFKYERDSNYHLLM----------SVQESLERKFGKHGGTIPIVPTAEFQDRISGAS Bovine
GRLTFKYERDSNYHLLM----------SVQESLERKFGKHGGTIPIVPTAEFQDRISGAS Human
GRLTFKYERDSNYHLLM----------SVQESLERKFGKHGGTIPVVPTAEFQDRISGAS Chicken
GRLTFKYERDSNYHLLM----------SVQESLERKFGKHGGAIPVVPTSEFQARIAGAS Om
GRLTFKYERESNYHLLE----------SVQESLERRFGRVGGRIPVTPSESFQKRISGAS Dm
GRLTFKYERESNYHLLASVQQSIERIINDESVQESLERRFGRVGGRIPVTPSESFQKRISGAS Dm2
GRLTFKYERESNYHLLE----------SVQRSLEARFGTVGGKIPIEASEAFKKRISGAS Ag
GRLSFKYEEDSNRMLLQ----------SVQDSLEKALNKEA---PVHPNDEFTARIAGAS Hc
GRLTFKYDEEANKMLLA----------SVQESLSKAVGK---DCPVEPNAAFAAKIAGAS Ce
GRMTRRWEETSKYKLLE----------AIQIST-------GLRVDVTKNQQAAKLLEGPS Pt
```

[a] The abbreviations Om, Dm, Ag, Hc, Ce, and Pt represent *Oncorhynchus mykiss*, *Drosophila melanogaster*, *Anopheles gambiae*, *Haemonchus contortus*, *Caenorhabditis elegans*, and *Paramecium tetraurelia*, respectively. Note that there are two different forms of *D. melanogaster* GDH with different sizes of antennae. The numbering at the top corresponds to the boGDH sequence. Identical residues are highlighted in yellow.

Table 4: Alignment of Those Residues Lining the GTP Binding Pocket As Defined Using the Program MS (*31*, *32*) and a 1.5 Å Probe Radius[a]

| | 209 | 210 | 212 | 213 | 217 | 257 | 258 | 261 | 262 | 265 | 289 | 292 | 446 | 450 |
|---|---|---|---|---|---|---|---|---|---|---|---|---|---|---|
| bovine | H | G | I | S | R | L | H | R | Y | R | K | E | K | H |
| human | H | G | I | S | R | L | H | R | Y | R | K | E | K | H |
| chicken | H | G | I | S | R | L | H | R | Y | R | K | E | K | H |
| *O. mykiss* | H | G | I | S | R | M | H | R | Y | R | K | E | K | H |
| *H. contortus* | H | G | V | S | R | L | H | R | Y | R | K | E | K | H |
| *C. elegans* | H | G | V | S | R | L | H | R | Y | R | K | E | K | H |
| *D. melanogaster* | H | G | V | S | R | L | H | R | Y | R | K | E | K | H |
| *A. gambiae* | H | G | V | S | R | L | H | R | Y | R | K | E | K | H |
| *P. tetraurelia* | S | G | T | E | L | Y | Y | K | Y | A | D | Q | K | F |
| *Arabidopsis thaliana* | S | L | T | E | Y | M | H | E | K | A | A | R | E | E |
| *Pyrococcus furiosus* | L | G | I | E | R | Y | Y | K | I | E | D | L | E | R |
| *Clostridium symbiosum* | L | V | P | E | Y | W | G | K | K | E | N | L | E | D |

[a] The sequence numbering is according to bovine GDH.

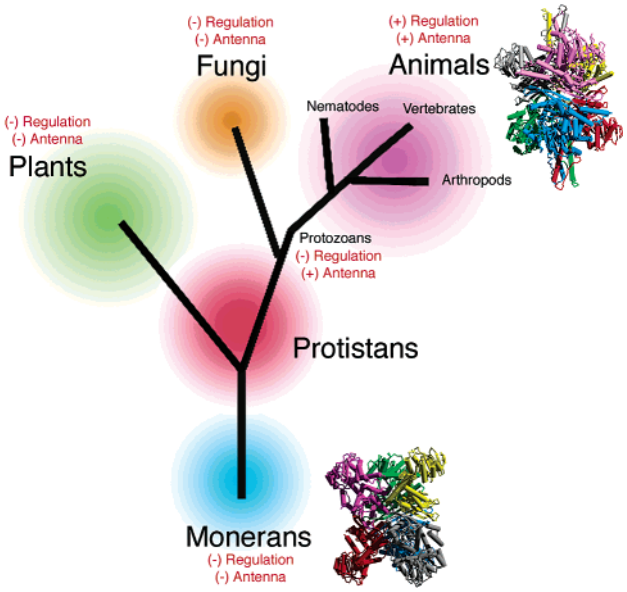


FIGURE 6: Schematic of the evolution of the antenna and purine regulation of GDH. On the basis of structural and sequence alignments, it is apparent that the antenna appeared in the protozoans before purine regulation. Subsequently, both the antenna and purine regulation are found in all animal species.

gous in this ADP binding pocket. If ADP does not bind to this region of paramecium GDH, it would be most likely due to more subtle changes in the pocket. For example, $_{b}$V492 lies directly under the ribose-binding pocket. The His in paramecium GDH at this position would likely be too large and would occlude at least some of this site. Similarly, an Arg at the S393 position would likely interfere with the binding of the $\beta$-phosphate even though it has a complementary charge. In addition, Gln at the K387 position would probably decrease interaction with the α-phosphate, and the Thr at the K488 position would not be able to interact as strongly with the ribose hydroxyl. In GDH from the remaining three kingdoms, similar loss of interactions and an increase in the bulkiness of the side chains may interfere with ADP binding. For example, all three have replaced $_{b}$R396 that interacts with the $\beta$-phosphate with a hydrophobic residue and $_{b}$H85 that interacts with the adenosine ring with an alanine.

## DISCUSSION

From electron microscopy results, it was suggested that boGDH forms long fibers by end-to-end association of the hexamers (*36*). Interestingly, boGDH forms similar fibers in the crystal cell, but these fibers differ between the apo and abortive complex forms (Figure 1). The interactions among the apo hexamers are more extensive than those found in crystals of the closed form. It is important to note that the polymers found in the apo boGDH structure are similar to those observed in TEM experiments (*37*).

If these polymers are truly indicative of the kinds of fibers found in solution, then these results could explain the effects

Table 5: Alignment of Those Residues Involved in the ADP Binding Pocket As Defined Using the Program MS (*31*, *32*) and a 1.5 Å Probe Radius[a]

| | 85 | 86 | 112 | 116 | 119 | 120 | 121 | 122 | 382 | 455 | 459 | 488 | 491 | 492 | 203 | 204 | 206 | 207 | 209 | 387 | 392 | 393 | 396 | 445 |
|---|---|---|---|---|---|---|---|---|---|---|---|---|---|---|---|---|---|---|---|---|---|---|---|---|
| bovine | Q | R | T | A | D | V | P | F | Y | Y | R | K | R | V | *I* | *S* | *G* | *G* | *H* | *K* | *V* | *S* | *R* | *E* |
| human | H | R | T | A | D | V | P | F | Y | Y | R | K | K | V | *I* | *S* | *G* | *G* | *H* | *K* | *V* | *S* | *R* | *E* |
| chicken | Q | R | T | A | D | V | P | F | A | Y | R | K | K | V | *I* | *S* | *G* | *G* | *H* | *K* | *V* | *S* | *R* | *E* |
| *O. mykiss* | H | R | T | A | D | V | P | F | Y | Y | R | K | K | V | *I* | *S* | *G* | *G* | *H* | *K* | *V* | *S* | *R* | *E* |
| *H. contortus* | H | R | T | A | D | V | P | F | Y | Y | R | K | N | T | *I* | *S* | *G* | *G* | *H* | *K* | *V* | *S* | *R* | *E* |
| *C. elegans* | H | R | T | A | D | V | P | F | Y | Y | R | K | N | T | *I* | *S* | *G* | *G* | *H* | *K* | *V* | *S* | *R* | *E* |
| *D. melanogaster* | H | K | T | A | D | V | P | F | F | Y | R | K | T | T | *I* | *N* | *G* | *G* | *H* | *K* | *V* | *S* | *R* | *E* |
| *A. gambiae* | H | R | T | A | D | V | P | F | F | Y | R | K | Q | T | *I* | *N* | *G* | *G* | *H* | *K* | *V* | *S* | *R* | *E* |
| *P. tetraurelia* | H | R | T | A | E | L | P | Y | Y | E | R | T | Q | H | *I* | *S* | *G* | *G* | *S* | *Q* | *I* | *R* | *R* | *A* |
| *A. thaliana* | A | L | T | A | P | Y | K | L | E | E | Q | N | Q | A | *I* | *Y* | *A* | *A* | *S* | *R* | *M* | *Q* | *A* | *E* |
| *P. furiosus* | A | R | T | A | D | L | P | Y | Y | K | K | R | Q | A | *L* | *S* | *G* | *G* | *L* | *Q* | *Y* | *Y* | *I* | *E* |
| *C. symbiosum* | A | I | A | S | T | L | P | M | G | Q | D | K | D | A | *R* | *S* | *G* | *G* | *L* | *Q* | *L* | *S* | *A* | *E* |

[a] The sequence numbering is according to bovine GDH. The residues on the right in italic type are those found in the adjacent subunit.

of GTP on the polymerization state of GDH. In the presence of ADP, the catalytic mouth is more likely to be "open", allowing for more extensive interactions between the antenna of one hexamer and both the NAD binding domain and antenna of the adjacent hexamer. In contrast, when GTP is added, the closed mouth conformation is stabilized. Therefore, the NAD binding domain is no longer available for this interaction, and this would decrease the tendency of the enzyme to polymerize. While it has been shown that this polymerization state is unrelated to catalytic activity (*38*, *39*), it seems rather coincidental that these antagonistic allosteric regulators also have opposing effects on enzyme polymerization. It may be that this polymerization process has some important role in the crowded environment of the mitochondria such as the formation of multienzyme complexes. It has been suggested that GDH is loosely associated with mitochondrial membranes (*40*). Therefore, this polymerization process may also somehow regulate this distribution of the enzyme within the mitochondria.

The differences in NAD binding domain orientations among the 12 subunits in the crystallographic asymmetric unit infer that it is in a highly mobile state when the catalytic cleft is open. Interestingly, this alignment also shows that these differences in the NAD binding domain orientations are correlated with differences in antenna conformations. These results imply that, as individual subunits open and close, the associated antennae also move with respect to the other antennae within the trimers. It is not clear, however, how larger conformational differences between the subunits are reconciled within the antenna but supports the contention that the antenna is responsible for the subunit communication associated with negative cooperativity (*3*, *15*).

While the binding interactions between GTP and its allosteric site are dominated by interactions with the triphosphate moiety (*2*, *15*), ADP appears to mainly bind via adenosine interactions. Previous studies demonstrated that the $_{h}$R463A mutation in huGDH abrogated ADP activation (*21*). To explain this result, it was suggested that ADP activates by interacting with $_{h}$R463 as the mouth opens. This would, in turn, make it easier for the enzyme to open the catalytic cleft and release product. It was assumed, and now shown here with this huGDH $_{h}$R463A mutant structure, that this mutation does not affect the structure of the ADP binding pocket. This is in contrast to what was found with GTP where the binding site is only available in the closed conformation (*2*). This concurs with the previous hypothesis that GTP only recognizes the closed conformation and locks the enzyme into this state whereas ADP can bind to either state and acts by decreasing the energy required to open the catalytic cleft (*2*). These studies also lend a physical model as to how ADP can alleviate abortive complexes (*10*).

It has been shown that NADH binds to a second site on the enzyme and causes inhibition (*17*). However, the mechanism of inhibition has been difficult to understand since $NAD^+$ has been suggested to bind to the same site and cause activation (*19*). There are several possible reasons for the differences between the conformations of the bound ADP and NAD(H) molecules. The most obvious difference is the presence of the nicotinamide ribose moiety. In both conformations of the bound NAD(H), extensive interactions with the enzyme could impose constraints on the adenosine ribose orientations such that these groups might be unable to bind with optimal contacts. Perhaps just as important, the enzyme is in the closed conformation in all of these NAD(H) complexes. The observed differences could also be due to the changes in the binding environment resulting from movement of the pivot helix.

With this structure of the GDH·ADP complex, the effects of NAD(H) bound to the second coenzyme site still remain unclear. Shafer et al. (*41*) showed that NADH alone binds with a stoichiometry of seven to eight molecules per hexamer. Glutamate and GTP both enhanced NADH affinity and increased the stoichiometry to 12 per hexamer (*13*). Since GTP and NADH bind synergistically and GTP only binds to the closed mouth conformation, these results suggest that NAD(H) mainly binds to the second coenzyme site when the catalytic mouth is closed. Also, since NADH binds synergistically with GTP (*13*) and the reaction is inhibited by high concentrations of NADH (*17*), the inference is that NADH binding to the second site is inhibitory. However, while the binding of NADH to this second site has a $K_d$ of $\sim$60 $\mu$M (*17*), NADH inhibition of the steady-state reaction is only observed at concentrations above 1 mM (*17*, *42*, *43*).

In an apparent contradiction to the notion that NADH binds to this site and causes inhibition are the results from studies on hysteretic phenomena observed in the reductive amination, steady-state reaction in the presence of GTP (*44*). In the presence of 50 $\mu$M GTP and using NADH as coenzyme, there is a time-dependent increase in the steady-state reaction velocity. This phenomenon is not observed when NADPH is used as coenzyme. When $NAD^+$ was added to the reaction, an increase in the initial reaction velocity was observed. It

was concluded that this activation process was due to $NAD^+$ binding to the ADP site and mimicking its activation by relieving GTP inhibition. This was consistent with previous spectroscopic studies showing that $NAD^+$ binding to the second coenzyme site induced conformational changes similar to ADP (*19*). Current kinetic data suggest, therefore, that the oxidation state of the coenzyme bound to this site determines whether it activates or inhibits the reaction. However, structural studies failed to find significant differences between the bound conformations of $NAD^+$ and NADH (*2*). With the ADP and second NAD(H) sites now clearly described, future site-directed mutagenesis studies will address this apparent paradox.

From sequence alignments of GDH from various sources, it appears that the antenna evolved before purine regulation as some of the protista started to evolve into multicellular animals. The antenna could not have evolved in response to the development of the mitochondria since neither fungi nor plants have this feature. Previous studies that demonstrated that antenna mutations affect GTP inhibition (*45*) imply that the antenna facilitates allosteric regulation. However, since paramecia have antennae but lack purine regulation, it appears that the antenna was not introduced for heterotrophic allosteric regulation. The rate-limiting step of the reaction is most likely the opening of the catalytic cleft via movement of the NAD binding domain, and it has been proposed that the motion of one subunit affects adjacent subunits via the antenna (*3*). It may be that antenna-mediated subunit communication transfers the mechanical energy involved in NAD binding domain movement to adjacent subunits in order to make catalytic turnover more efficient. If true, then it follows that the negative cooperativity observed in animal GDH is a consequence of antenna communication and exists to improve catalytic efficacy.

Purine regulation is likely to have evolved to give GDH several unique functions in animals. The most obvious difference between animals and the other kingdoms is that animals experience more rapid changes in environment and nutrient uptake. Plants, for example, upregulate transcription of GDH in response to high soil levels of ammonium to both prevent toxicity and facilitate nitrogen transport (*46*). Animals, in contrast, need a more energy-efficient, faster, and more subtle response to changes in amino acid availability and energy needs than transcriptional regulation. The importance of this regulation was made evident in the case of hyperinsulinism where the loss of GTP inhibition causes uncontrolled secretion of insulin (*35*). In addition, this syndrome and recent structural results suggest that GDH in animals may be a major "energy sensing" conduit linking protein catabolism and ATP generation (*2*, *3*), and therefore rapid and fine-tuned regulation is necessary. Additional support for the role of GDH in insulin homeostasis has come from recent findings that leucine induces $\beta$-cell secretion of insulin through activation of GDH (*47*). Finally, a use for GDH unique to animals is in the regulation of glutamate in its role as a neurotransmitter. Only allosteric regulation of GDH can provide fast enough response to the changing levels of glutamate during neural transmission. Together, these results suggest that, rather than create several new genes to accommodate growing regulatory needs, animals made subtle changes in this ancient enzyme.

## ACKNOWLEDGMENT

The program MolView [(*48*) http://www.danforthcenter-.org/smith/] was used to create Figures 1A, 2, 3, 4, and 5. The program GRASP (*49*) was used to make Figure 1B,C.

## REFERENCES

1. Peterson, P., Pierce, J., and Smith, T. J. (1998) *J. Struct. Biol. 120*, 73−77.
2. Smith, T. J., Peterson, P. E., Schmidt, T., Fang, J., and Stanley, C. (2001) *J. Mol. Biol. 307*, 707−720.
3. Smith, T. J., Schmidt, T., Fang, J., Wu, J., Siuzdak, G., and Stanley, C. A. (2002) *J. Mol. Biol. 318*, 765−777.
4. Knapp, S., de Vos, W. M., Rice, D., and Ladenstein, R. (1997) *J. Mol. Biol. 267*, 916−932.
5. Rice, D. W., Baker, P. J., Farrants, G. W., and Hornby, D. P. (1987) *Biochem. J. 242*, 789−795.
6. Yip, K. S. P., Stillman, T. J., Britton, K. L., Artymiuk, P. J., Baker, P. J., Sedelnikova, S. E., Engel, P. C., Pasquo, A., Chiaraluce, R., Consalvi, V., Scandurra, R., and Rice, D. W. (1995) *Structure 3*, 1147−1158.
7. Stillman, T. J., Baker, P. J., Britton, K. L., and Rice, D. W. (1993) *J. Mol. Biol. 234*, 1131−1139.
8. Colman, R. F. (1991) in *A Study of Enzymes* (Kuby, S. A., Ed.) pp 173−192, CRC Press, New York.
9. Frieden, C. (1965) *J. Biol. Chem. 240*, 2028−2037.
10. George, S. A., and Bell, J. E. (1980) *Biochemistry 19*, 6057−6061.
11. Iwatsubo, M., and Pantaloni, D. (1967) *Bull. Soc. Chem. Biol. 49*, 1563−1572.
12. Bailey, J. S., Bell, E. T., and Bell, J. E. (1982) *J. Biol. Chem. 257*, 5579−5583.
13. Koberstein, R., and Sund, H. (1973) *Eur. J. Biochem. 36*, 545−552.
14. Dieter, H., Koberstein, R., and Sund, H. (1981) *Eur. J. Biochem. 115*, 217−226.
15. Peterson, P. E., and Smith, T. J. (1999) *Structure 7*, 769−782.
16. Frieden, C. (1959) *J. Biol. Chem. 234*, 809−814.
17. Frieden, C. (1959) *J. Biol. Chem. 234*, 815−819.
18. Limuti, C. M. (1983) Ph.D. Thesis, Department of Biochemistry, University of Rochester, Rochester, New York.
19. Bayley, P. M., and O'Neill, T. J. (1980) *Eur. J. Biochem. 112*, 521−531.
20. Wrzeszczynski, K. O., and Colman, R. F. (1994) *Biochemistry 33*, 11544−11553.
21. Fang, J., Macmullen, C., Smith, T. J., and Stanley, C. A. (2001) *Biochem. J. 363*, 81−87.
22. Weinzimer, S. A., Stanley, C. A., Berry, G. T., Yudkoff, M., Tuchman, M., and Thornton, P. S. (1997) *J. Pediatr. 130*, 661−664.
23. Cheung, V. G., Gregg, J. P., Gogolin-Ewens, K. J., Bandong, J., Stanley, C. A., Baker, L., Higgins, M. J., Nowak, N. J., Shows, T. B., Ewens, W. J., Nelson, S. F., and Spielman, R. S. (1998) *Nat. Genet. 18*, 225−230.
24. Matthews, B. W. (1968) *J. Mol. Biol. 33*, 491−497.
25. Brunger, A. T., Adams, P. D., Clore, G. M., Gros, P., Grosse-Kunstleve, R. W., Jiang, J.-S., Kuszewski, J., Nilges, N., Pannu, N. S., Read, R. J., Rice, L. M., Simonson, T., and Warren, G. L. (1998) *Acta Crystallogr. D 54*, 905−921.
26. Olsen, J. A., and Anfinsen, C. B. (1952) *J. Biol. Chem. 197*, 67−79.
27. Frieden, C. (1958) *Biochim. Biophys. Acta 27*, 431−432.
28. Chun, P. W., Kim, S. J., Stanley, C. A., and Ackers, G. K. (1969) *Biochemistry 8*, 1625−1632.
29. Colman, R. F., and Frieden, C. (1966) *Biochem. Biophys. Res. Commun. 22*, 100−105.
30. Connolly, M. L. (1981) Ph.D. Thesis, University of California, Berkeley, Berkeley, CA.
31. Connolly, M. L. (1983) *J. Appl. Crystallogr. 16*, 548.
32. Connolly, M. L. (1983) *Science 221*, 709.
33. Altschul, S. F., Madden, T. L., Schäffer, A. A., Zhang, J., Zhang, Z., Miller, W., and Lipman, D. J. (1997) *Nucleic Acids Res. 25*, 3389−3402.
34. Papadopoulou, D., and Louis, C. (2000) *J. Neurogenet. 14*, 125−143.

35. Stanley, C. A., Lieu, Y. K., Hsu, B. Y. L., Burlina, A. B., Greenberg, C. R., Hopwood, N. J., Perlman, K., Rich, B. H., Zammarchi, E., and Poncz, M. (1998) *N. Engl. J. Med. 338*, 1352−1357.
36. Eisenberg, H., and Reisler, E. (1970) *Biopolymers 9*, 113−115.
37. Josephs, R., and Borisy, G. (1972) *J. Mol. Biol. 65*, 127−155.
38. Fisher, H. F., Cross, D., and McGregor, L. L. (1962) *Nature 196*, 895−896.
39. Josephs, R., Eisenberg, H., and Reisler, E. (1973) *Biochemistry 12*, 4060−4067.
40. Yamaya, T., and Oaks, A. (1987) *Physiol. Plant 70*, 749−756.
41. Shafer, J. A., Chiancone, E., Vittorelli, L. M., Spagnuolo, C., Machler, B., and Antonini, E. (1972) *Eur. J. Biochem. 31*, 166−171.
42. Batra, S. P., and Colman, R. F. (1986) *Biochemistry 25*, 3508−3515.
43. Batra, S. P., and Colman, R. F. (1984) *Biochemistry 23*, 4940−4946.
44. Smith, T. J., and Bell, J. E. (1982) *Biochemistry 21*, 733.
45. Stanley, C. A., Fang, J., Kutyna, K., Hsu, B. Y., Ming, J. E., Glaser, B., and Poncz, M. (2000) *Diabetes 49*, 667−673.
46. Frechilla, S., Lasa, B., Aleu, M., Juanarena, N., Lamsfus, C., and Aparicio-Tejo, P. M. (2002) *J. Plant Phys. 159*, 811−818.
47. Li, C., Najafi, H., Daikhin, Y., Nissim, I., Collins, H. W., Yudkoff, M., Matschinsky, F. M., and Stanley, C. A. (2003) *J. Biol. Chem.* (in press).
48. Smith, T. J. (1995) *J. Mol. Graphics 13*, 122−125.
49. Nicholls, A. (1993) Ph.D. Thesis, Columbia University, New York.

BI0206917